THE JOURNAL OF PHYSICAL CHEMISTRY A

Article

Dependence of the Two-Photon Absorption Cross Section on the Conjugation of the Phenylacetylene Linker in Dipolar Donor–Bridge–Acceptor Chromophores

Soohyun Lee, K. R. Justin Thomas, S. Thayumanavan, and Christopher J. Bardeen

J. Phys. Chem. A, **2005**, 109 (43), 9767-9774 • DOI: 10.1021/jp053864l

Dependence of the Two-Photon Absorption Cross Section on the Conjugation of the Phenylacetylene Linker in Dipolar Donor−Bridge−Acceptor Chromophores

Soohyun Lee,[†] K. R. Justin Thomas,[‡] S. Thayumanavan,[‡] and Christopher J. Bardeen*,[†]

Departments of Chemistry, University of California, Riverside, California 92521, and University of Massachusetts, Amherst, Massachusetts 01003

Received: July 13, 2005; In Final Form: August 31, 2005

The nonlinear optical properties of four isomeric dipolar two-photon chromophores are compared. The chromophores consist of a carbazole electron donor coupled to a naphthalimide electron acceptor by a phenylacetylene bridge. By variation of the connectivity of the bridge at the phenyl groups, four compounds with 0, 1, and 2 *meta* linkages are synthesized. The linear and nonlinear optical properties of these compounds are measured. Despite similar linear absorption cross sections, the two-photon absorption cross section δ of the all-*meta* compound is almost a factor of 10 lower than the all-*para* compound. By taking the detailed molecular conformations into account in order to calculate accurate dipole moment changes, we find that the decrease in δ results largely from the decreased charge transfer ability with increasing number of meta linkages. We find that a two-state model can be used to predict semiquantitatively the observed trend in δ on the basis of the linear optical properties of the molecules. This work illustrates the dramatic effect the ground-state polarizability can have on the nonlinear optical response of organic compounds and also provides a way to quantify the ability of *meta* linkages to inhibit charge transfer in their ground-state configuration.

Introduction

The development of new nonlinear optical materials is driven by their diverse applications, ranging from optical switching to biological imaging. Polarizable organic molecules can have very high nonlinear optical coefficients and have the advantage that organic synthesis can be used to tune their properties in a variety of ways. Furthermore, the theoretical understanding of the electronic properties of large organic molecules has advanced to the point where relative trends and even absolute nonlinearities can be predicted with a high degree of confidence.[1−4] As a specific example, the third-order molecular nonlinearity which results in two-photon absorption has been the subject of numerous studies. Two-photon absorption occurs when two nonresonant, low-energy photons are simultaneously absorbed to produce a high-energy excited state. In general, this phenomenon requires high light intensities and occurs only at the focus of a laser beam. This optical nonlinearity can be technologically useful when the excited state produces a desired outcome. For example, if the excited state is chemically active, one can take advantage of the spatially localized excitation to create three-dimensional structures for data storage,[5−7] photolithography,[8−13] or other types of photosensitization.[14,15] If, on the other hand, the excited state has a high fluorescence quantum yield, then the localized excitation allows one to perform high-resolution confocal microscopy using laser wavelengths not directly absorbed by the sample.[16] This second aspect of two-photon absorption has proved to be especially useful in biological microscopy.[17,18] Two-photon chromophores provide a good example of how the combination of organic synthesis and quantum mechanical calculations can lead to rapid advances in nonlinear optical materials. Recent work has shown how two-photon absorption cross sections can be improved by orders of magnitude within a class of molecules by systematically changing different structural parts.[19−23] The experimental results are supported by extensive theoretical work,[24−29] which shows quantitatively how changing the various aspects of molecular structure affects the two-photon cross section δ.

In the simplest type of two-photon absorber, the chromophore has a single electron donor and acceptor group, covalently linked by a molecular bridge. This asymmetrical dipolar compound is distinguished from quadrapolar and octopolar compounds where multiple donors are arranged symmetrically around a central acceptor.[21] Although such symmetrical compounds have demonstrated the highest nonlinearities, the simpler structure of dipolar compounds makes them useful for studying the fundamental details of how molecular structure impacts the two-photon absorption process. In this paper, we are concerned with determining the influence of bridge conjugation on the two-photon absorption properties of model donor−bridge−acceptor (DBA) compounds. We have synthesized molecules where the electron donor (a carbazole group) is connected to the acceptor (a naphthalimide moiety) by a phenylacetylene (PA) bridge containing two phenyl rings. By altering the branching at each phenyl ring, we create a set of four isomeric bridges with varying geometries. These different donor−bridge−acceptor structures are shown in Figure 1. By measuring the two-photon absorption cross section in these molecules relative to a standard, we find a dramatic dependence on bridge structure, with the cross section of the all-*meta* bridge being almost a factor of 10 lower than that of the all-*para* bridge. Comparison of our experimental results with analytical predictions on the basis of a two-state model for dipolar compounds shows that this model is able to semiquantitatively reproduce the observed trends. To achieve this agreement, the details of the molecular conformations must be explicitly taken into account. Our results provide a dramatic

* To whom correspondence should be addressed. E-mail: christopher.bardeen@ucr.edu.
[†] University of California.
[‡] University of Massachusetts.

10.1021/jp053864l CCC: $30.25
Published on Web 10/08/2005

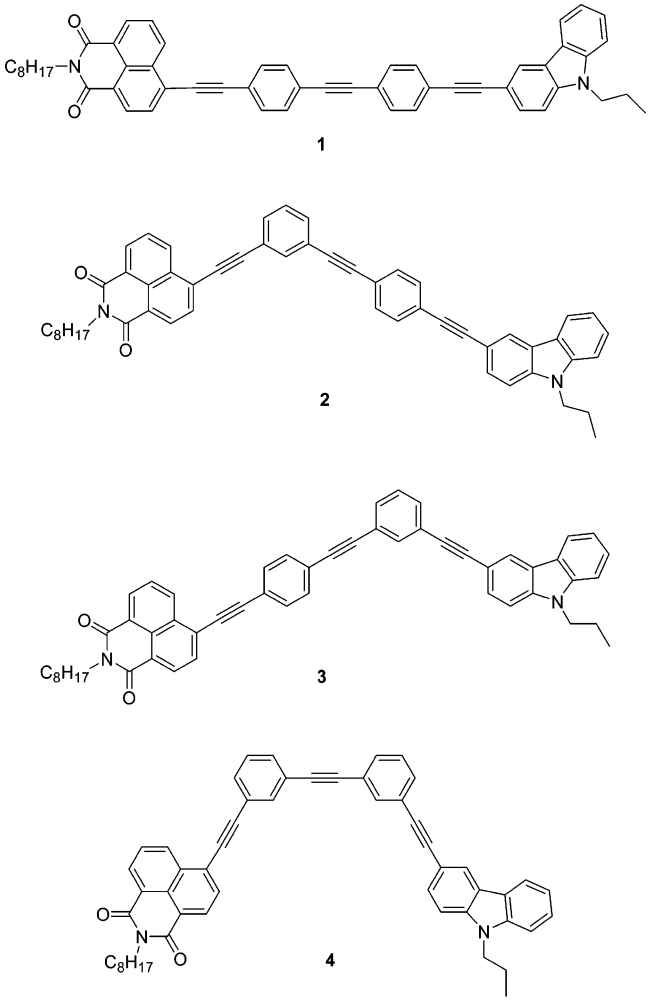

Figure 1. Molecular structures of molecules **1**−**4**.

SCHEME 1: Synthesis of Molecules 1−4 Part 1

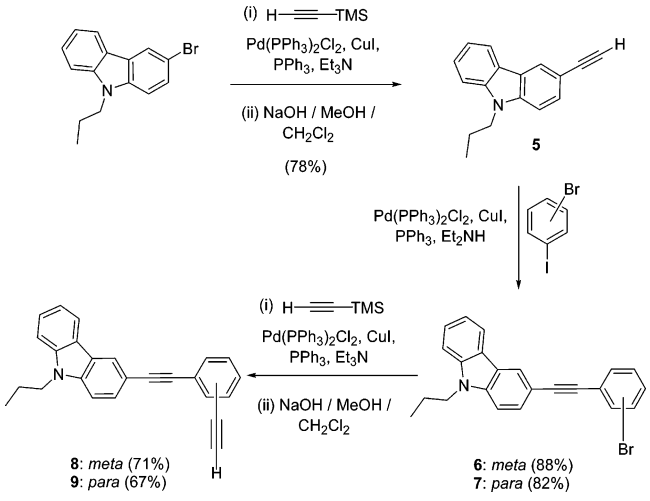

experimental demonstration of the importance of the ground-state polarizability in determining the strength of the molecular nonlinear optical response.

Experimental Section

Synthesis of Molecules 1−4. The synthesis of molecules **1**−**4** is outlined in Schemes 1 and 2. Details are given below. All starting materials were purchased from commercial sources and were used without further purification, unless mentioned otherwise. The following chemicals were prepared according to literature procedures: 9-propyl-9*H*-carbazole;[30] 3,6-dibromo-9-propyl-9*H*-carbazole;[30] 5-bromo-*N*-octyl-1,8-naphthalimide.[31] All solvents used for reactions were dried according to standard procedures and freshly distilled prior to use. Solvents for extraction were obtained from commercial sources (ACS grade) and used as received. Flash chromatography was run on 230−400 mesh silica gel (Merck). NMR spectra were recorded in $CDCl_3$ using a Bruker DPX300 spectrometer operating at 300 MHz for proton and 75 MHz for carbon-13 at a temperature of 293 K. Mass spectrometry was performed at the JMS700 MStation (FAB mass) or Bruker Daltonics Reflex III (MALDI-TOF). The synthesis is outlined in Schemes 1 and 2, and the detailed procedures are given below.

3-Ethynyl-9-propyl-9*H*-carbazole (5). A mixture of 3-bromo-9-propyl-9*H*-carbazole (2.88 g, 10 mmol), (trimethylsilyl)-acetylene (1.18 g, 12 mmol), $Pd(PPh_3)_2Cl_2$ (70 mg, 0.1 mmol), CuI (19 mg, 0.1 mmol), triphenylphosphine (53 mg, 0.2 mmol), and triethylamine (50 mL) was heated at 70 °C for 18 h. The volatiles were removed, and the residue was dissolved in diethyl ether and passed through a short silica gel column. The eluant obtained containing the intermediate, 3-(2-(trimethylsilyl)-ethynyl)-9-propyl-9*H*-carbazole, was concentrated to dryness and redissolved in dichloromethane/methanol mixture (1:2). It was treated with sodium hydroxide, 0.40 g (10 mmol), overnight. The reaction was quenched by the addition of water, and the organic product was extracted into diethyl ether. The ethereal extract was dried over anhydrous $MgSO_4$ and evaporated to yield the crude product. It was further purified by column chromatography using hexane/dichloromethane mixture (4:1) as eluant. Yield: 1.82 g (78%) of a colorless solid. ^{1}H NMR [δ ($CDCl_3$)]: 0.99 (t, J = 7.3 Hz, 3 H), 1.87−1.99 (m, 2 H), 3.11 (s, 1 H), 4.28 (t, J = 7.3 Hz, 2 H), 7.26 (t, J = 7.0 Hz, 1 H), 7.33 (d, J = 8.5 Hz, 1 H), 7.40 (d, J = 8.1 Hz, 1 H), 7.49 (t, J = 8.1 Hz, 1 H), 7.62 (dd, J = 8.5, 1.5 Hz, 1 H), 8.11 (d, J = 7.7 Hz, 1 H), 8.30 (d, J = 1.5 Hz, 1 H). ^{13}C NMR [δ ($CDCl_3$)]: 140.9, 140.4, 129.6, 126.2, 124.7, 122.7, 122.4, 119.4, 112.0, 109.0, 108.8, 85.2, 75.2, 44.7, 22.3, 11.8. MS (EI; *m*/*z*): 233.116 (M^+).

3-((3-Bromophenyl)ethynyl)-9-propyl-9*H*-carbazole (6). A mixture of 3-ethynyl-9-propyl-9*H*-carbazole (2.33 g, 10 mmol), 1-bromo-3-iodobenzene (3.96 g, 14 mmol), $Pd(PPh_3)_2Cl_2$ (70 mg, 0.1 mmol), CuI (19 mg, 0.1 mmol), triphenylphosphine (53 mg, 0.2 mmol), and diethylamine (50 mL) was stirred at room temperature for 18 h. After removal of the solvent the residue was adsorbed on silica gel and purified by column chromatography to yield the title compound as a colorless solid (3.42 g, 88%). ^{1}H NMR [δ ($CDCl_3$)]: 0.95 (t, J = 7.3 Hz, 3 H), 1.87−1.95 (m, 2 H), 4.25 (t, J = 7.3 Hz, 2 H), 7.11−7.28 (m, 2 H), 7.33−7.51 (m, 5 H), 7.62 (dd, J = 8.3, 1.1 Hz, 1 H), 7.73−7.74 (m, 1 H), 8.09 (d, J = 7.7 Hz, 1 H), 8.29 (d, J = 1.1 Hz, 1 H). ^{13}C NMR [δ ($CDCl_3$)]: 140.8, 140.3, 134.1, 130.8, 129.9, 129.7, 129.2, 126.1, 126.0, 124.1, 122.8, 122.3, 122.1, 120.5, 119.4, 112.5, 109.0, 108.8, 92.3, 86.1, 44.7, 22.3, 11.8. MS (EI; *m*/*z*): 387.05 (M^+).

3-((4-Bromophenyl)ethynyl)-9-propyl-9*H*-carbazole (7). It was prepared as described above from 3-ethynyl-9-propyl-9*H*-carbazole and 1-bromo-4-iodobenzene in 82% yield (colorless solid). ^{1}H NMR [δ ($CDCl_3$)]: 0.97 (t, J = 7.3 Hz, 3 H), 1.84−1.97 (m, 2 H), 4.24 (t, J = 7.3 Hz, 2 H), 7.27 (t, J = 7.7 Hz, 1 H), 7.34−7.52 (m, 7 H), 7.63 (dd, J = 8.3, 1.1 Hz, 1 H), 8.10 (d, J = 7.7 Hz, 1 H), 8.30 (d, J = 1.1 Hz, 1 H). ^{13}C NMR [δ ($CDCl_3$)]: 140.9, 140.3, 132.8, 131.5, 129.1, 126.1, 124.0, 122.9, 122.8, 122.4, 121.8, 120.5, 119.4, 112.8, 109.0, 108.8, 92.4, 86.5, 44.7, 22.3, 11.7. MS (EI; *m*/*z*): 387.06 (M^+).

SCHEME 2: Synthesis of Molecules 1−4 Part 2

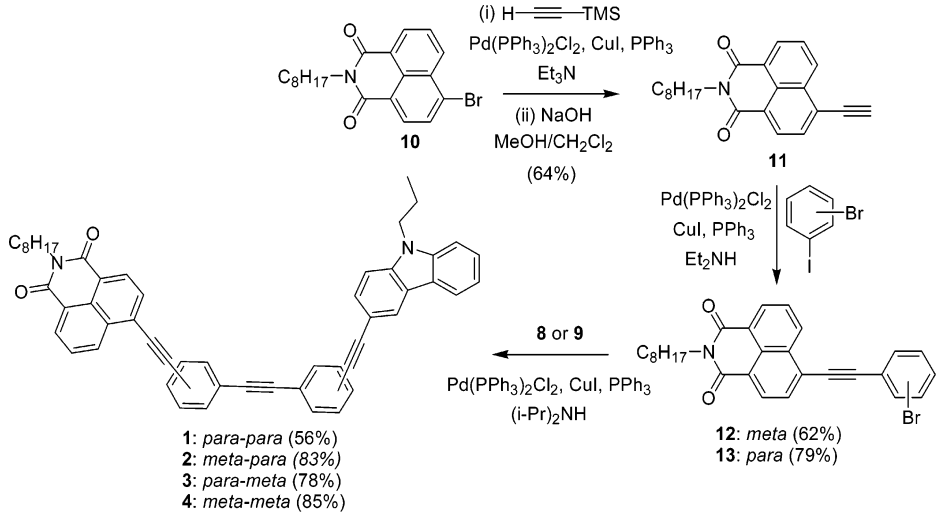

3-((3-Ethynylphenyl)ethynyl)-9-propyl-9*H*-carbazole (8). It was prepared from compound **6** and (trimethylsilyl)acetylene as described above for compound **5**. Yield: 71% of a colorless solid. ^{1}H NMR [δ ($CDCl_3$)]: 0.97 (t, J = 7.3 Hz, 3 H), 1.87−1.94 (m, 2 H), 3.12 (s, 1 H), 4.24 (t, J = 7.3 Hz, 2 H), 7.25−7.50 (m, 6 H), 7.56 (td, J = 7.7, 1.5 Hz, 1 H), 7.63 (dd, J = 8.5, 1.5 Hz, 1 H), 7.74 (t, J = 1.5 Hz, 1 H), 8.10 (d, J = 7.7 Hz, 1 H), 8.31 (d, J = 1.5 Hz, 1 H). ^{13}C NMR [δ ($CDCl_3$)]: 140.8, 140.2, 134.9, 131.7, 131.2, 129.2, 128.4, 126.1, 124.3, 124.1, 122.8, 122.3, 120.5, 119.3, 112.7, 109.0, 108.8, 91.7, 86.5, 83.0, 77.4, 44.6, 22.3, 11.7. MS (EI; *m*/*z*): 333.151 (M^+).

3-((4-Ethynylphenyl)ethynyl)-9-propyl-9*H*-carbazole (9). It was prepared from compound **7** and (trimethylsilyl)acetylene as described above for compound **5**. Yield: 67% Of a colorless solid. ^{1}H NMR [δ ($CDCl_3$)]: 0.94 (t, J = 7.3 Hz, 3 H), 1.84−1.96 (m, 2 H), 3.19 (s, 1 H), 4.24 (t, J = 7.3 Hz, 2 H), 7.27 (dt, J = 7.7, 1.5 Hz, 1 H), 7.34−7.42 (m, 2 H), 7.47−7.56 (m, 5 H), 7.63 (dd, J = 8.5, 1.5 Hz, 1 H), 8.10 (d, J = 7.7 Hz, 1 H), 8.31 (d, J = 1.5 Hz, 1 H). ^{13}C NMR [δ ($CDCl_3$)]: 140.8, 140.3, 132.0, 131.2, 129.2, 126.1, 124.5, 124.1, 122.8, 122.3, 121.2, 120.5, 119.4, 112.7, 109.0, 108.8, 93.1, 87.1, 83.4, 77.4, 44.6, 22.2, 11.7. MS (EI; *m*/*z*): 333.152 (M^+).

6-Ethynyl-2-octylbenzo[*de*]isoquinoline-1,3-dione (11). A mixture of 5-bromo-*N*-octyl-1,8-naphthalimide (3.88 g, 10 mmol), (trimethylsilyl)acetylene (1.18 g, 12 mmol), $Pd(PPh_3)_2Cl_2$ (70 mg, 0.1 mmol), CuI (19 mg, 0.1 mmol), triphenylphosphine (53 mg, 0.2 mmol), and triethylamine (50 mL) was heated at 70 °C for 18 h. The volatiles were removed, and the residue was dissolved in diethyl ether and passed through a short silica gel column. The eluant obtained containing the intermediate 2-octyl-6-(trimethylsilanyl)ethynylbenzo[*de*]isoquinoline-1,3-dione was concentrated to dryness and redissolved in dichloromethane/methanol mixture (1:2). It was treated with sodium hydroxide, 0.40 g (10 mmol), overnight. The reaction was quenched by the addition of water, and the organic product was extracted into diethyl ether. The ethereal extract was dried over anhydrous $MgSO_4$ and evaporated to yield the crude product. It was further purified by column chromatography using hexane/dichloromethane mixture (1:1) as eluant. Yield: 2.13 g (64%) of colorless solid. ^{1}H NMR [δ ($CDCl_3$)]: 0.86 (t, J = 7.3 Hz, 3 H), 1.24−1.39 (m, 10 H), 1.63−1.75 (m, 2 H), 3.71 (s, 1 H), 4.13 (t, J = 7.3 Hz, 2 H), 7.77 (t, J = 7.7 Hz, 1 H), 7.88 (d, J = 7.7 Hz, 1 H), 8.48 (d, J = 7.7 Hz, 1 H), 8.57−8.61 (m, 2 H). ^{13}C NMR [δ ($CDCl_3$)]: 163.8, 163.5, 142.1, 131.9, 130.1, 127.8, 127.6, 126.1, 123.0, 122.8, 86.4, 80.3, 40.6, 31.8, 29.3, 29.2, 28.1, 27.1, 22.6, 14.1. MS (EI; *m*/*z*): 333.171 (M^+).

6-((3-Bromophenyl)ethynyl)-2-octylbenzo[*de*]isoquinoline-1,3-dione (12). A mixture of 6-ethynyl-2-octylbenzo[*de*]isoquinoline-1,3-dione (3.33 g, 10 mmol), 1-bromo-3-iodobenzene (3.96 g, 14 mmol), $Pd(PPh_3)_2Cl_2$ (70 mg, 0.1 mmol), CuI (19 mg, 0.1 mmol), triphenylphosphine (53 mg, 0.2 mmol), and diethylamine (50 mL) was stirred at room temperature for 18 h. After removal of the solvent the residue was adsorbed on silica gel and purified by column chromatography to yield the title compound as colorless solid (3.03 g, 62%). ^{1}H NMR [δ ($CDCl_3$)]: 0.86 (t, J = 7.3 Hz, 3 H), 1.25−1.40 (m, 10 H), 1.65−1.75 (m, 2 H), 4.13 (t, J = 7.3 Hz, 2 H), 7.27 (t, J = 7.7 Hz, 1 H), 7.52−7.58 (m, 2 H), 7.77−7.82 (m, 2 H), 7.89 (d, J = 7.7 Hz, 1 H), 8.50 (d, J = 7.7 Hz, 1 H), 8.58−8.64 (m, 2 H). ^{13}C NMR [δ ($CDCl_3$)]: 163.8, 163.6, 134.5, 132.4, 132.0, 131.6, 131.5, 130.9, 130.4, 130.2, 130.0, 127.9, 127.5, 126.8, 124.2, 123.0, 122.5, 122.4, 97.0, 87.3, 40.6, 31.8, 29.3, 29.2, 28.1, 27.1, 27.1, 22.6, 14.1. MS (FAB; *m*/*z*): 487.111 (M^+).

6-((4-Bromophenyl)ethynyl)-2-octylbenzo[*de*]isoquinoline-1,3-dione (13). It was obtained in 79% yield as a colorless solid from 6-ethynyl-2-octylbenzo[*de*]isoquinoline-1,3-dione and 1-bromo-4-iodobenzene as described above for compound **12**. ^{1}H NMR [δ ($CDCl_3$)]: 0.86 (t, J = 7.3 Hz, 3 H), 1.25−1.39 (m, 10 H), 1.65−1.75 (m, 2 H), 4.13 (t, J = 7.3 Hz, 2 H), 7.44−7.56 (m, 4 H), 7.79 (t, J = 7.7 Hz, 1 H), 7.89 (d, J = 7.7 Hz, 1 H), 8.50 (d, J = 7.7 Hz, 1 H), 8.59 (d, J = 6.6 Hz, 1 H), 8.63 (d, J = 6.6 Hz, 1 H). ^{13}C NMR [δ ($CDCl_3$)]: 163.9, 163.6, 133.2, 132.1, 131.9, 131.6, 131.4, 130.8, 130.2, 128.0, 127.5, 127.0, 123.8, 123.0, 122.3, 121.1, 97.7, 87.3, 40.6, 31.8, 29.3, 29.2, 28.1, 27.1, 22.6, 14.1. MS (FAB; *m*/*z*): 487.113 (M^+).

2-Octyl-6-{((4-[4-((9-propyl-9*H*-carbazol-3-yl)ethynyl)-phenyl)ethynyl]phenyl)ethynyl}benzo[*de*]isoquinoline-1,3-dione (1). The title compound was obtained in 56% yield from **13** and **9** by following the standard Sonogashira protocol. A yellow solid formed. ^{1}H NMR [δ ($CDCl_3$)]: 0.86 (t, J = 7.3 Hz, 3 H), 0.97 (t, J = 7.3 Hz, 3 H), 1.26−1.41 (m, 10 H), 1.67−1.75 (m, 2 H), 1.88−1.95 (m, 2 H), 4.16 (t, J = 7.3 Hz, 2 H), 4.27 (t, J = 7.3 Hz, 2 H), 7.36−7.48 (m, 4 H), 7.51−7.67 (m, 9 H), 7.83 (t, J = 7.7 Hz, 1 H), 7.95 (d, J = 7.7 Hz, 1 H), 8.08 (d, J = 7.7 Hz, 1 H), 8.29 (d, J = 1.2 Hz, 1 H), 8.55 (d, J = 7.7 Hz, 1 H), 8.64 (dd, J = 7.7, 1.2 Hz, 1 H), 8.71 (dd, J = 8.5, 1.5 Hz, 1 H). ^{13}C NMR [δ ($CDCl_3$)]: 164.0, 163.8, 140.9, 140.3, 131.9, 131.8, 131.6, 131.4, 130.9, 130.3, 129.2,

128.1, 127.5, 127.2, 124.2, 124.1, 123.1, 122.9, 122.4, 122.3, 122.0, 121.9, 112.8, 109.0, 108.8, 93.3, 92.0, 90.4, 88.1, 87.3, 77.2, 44.8, 40.6, 31.8, 29.3, 29.2, 28.1, 27.2, 22.6, 22.3, 14.1, 11.8. MS (FAB; *m*/*z*): 741.0 (M^+). Anal. Calcd for $C_{53}H_{44}N_2O_2$: C, 85.91; H, 5.99; N, 3.78. Found: C, 86.29; H, 5.86; N, 3.66.

2-Octyl-6-{3-[((4-((9-propyl-9*H*-carbazol-3-yl)ethynyl)-phenyl)ethynyl]phenyl)ethynyl}benzo[*de*]isoquinoline-1,3-dione (2). The title compound was obtained in 83% yield from **12** and **9** by following the standard Sonogashira protocol. A yellow solid formed. ^{1}H NMR [δ ($CDCl_3$)]: 0.86 (t, J = 7.3 Hz, 3 H), 0.96 (t, J = 7.3 Hz, 3 H), 1.26−1.41 (m, 10 H), 1.67−1.77 (m, 2 H), 1.84−1.96 (m, 2 H), 4.15 (t, J = 7.3 Hz, 2 H), 4.24 (t, J = 7.3 Hz, 3 H), 7.24 (t, J = 7.7 Hz, 1 H), 7.33−7.39 (m, 3 H), 7.40−7.62 (m, 9 H), 7.78−7.83 (m, 2 H), 7.91 (d, J = 7.7 Hz, 1 H), 8.06 (d, J = 7.7 Hz, 1 H), 8.26 (d, J = 1.5 Hz, 1 H), 8.51 (d, J = 7.7 Hz, 1 H), 8.61 (d, J = 6.6 Hz, 1 H), 8.68 (d, J = 6.6 Hz, 1 H). ^{13}C NMR [δ ($CDCl_3$)]: 163.9, 163.7, 140.9, 140.3, 124.8, 132.4, 132.2, 131.6, 131.6, 131.4, 130.8, 130.3, 129.3, 128.8, 128.0, 127.5, 127.1, 126.2, 124.3, 124.1, 123.9, 123.0, 122.9, 122.7, 122.4, 122.3, 121.9, 120.5, 119.4, 112.8, 109.0, 108.8, 98.0, 93.3, 90.5, 89.8, 87.3, 86.9, 44.8, 40.6, 31.9, 29.4, 29.3, 28.2, 27.2, 22.7, 22.3, 14.1, 11.8. MS (FAB; *m*/*z*): 741.0 (M^+). Anal. Calcd for $C_{53}H_{44}N_2O_2$: C, 85.91; H, 5.99; N, 3.78. Found: C, 86.04; H, 6.14; N, 3.64.

2-Octyl-6-{4-[(3-((9-propyl-9*H*-carbazol-3-yl)ethynyl)-phenyl)ethynyl]phenyl)ethynyl}benzo[*de*]isoquinoline-1,3-dione (3). The title compound was obtained in 78% yield from **13** and **8** by following the standard Sonogashira protocol. A yellow solid formed. ^{1}H NMR [δ ($CDCl_3$)]: 0.86 (t, J = 7.3 Hz, 3 H), 0.97 (t, J = 7.3 Hz, 3 H), 1.25−1.41 (m, 10 H), 1.67−1.77 (m, 2 H), 1.84−1.97 (m, 2 H), 4.15 (t, J = 7.3 Hz, 2 H), 4.25 (t, J = 7.3 Hz, 2 H), 7.24 (t, J = 7.7 Hz, 1 H), 7.32−7.40 (m, 3 H), 7.45−7.50 (m, 2 H), 7.52−7.66 (m, 6 H), 7.76 (s, 1 H), 7.81 (t, J = 8.1 Hz, 1 H), 7.92 (d, J = 7.7 Hz, 1 H), 8.07 (d, J = 7.7 Hz, 1 H), 8.27 (d, J = 1.5 Hz, 1 H), 8.52 (d, J = 7.7 Hz, 1 H), 8.61 (dd, J = 6.6, 1.1 Hz, 1 H), 8.68 (dd, J = 6.6, 1.1 Hz, 1 H). ^{13}C NMR [δ ($CDCl_3$)]: 163.9, 163.6, 140.8, 140.3, 134.5, 132.2, 131.8, 131.7, 131.6, 131.5, 130.8, 130.7, 130.3, 129.2, 128.5, 128.0, 127.5, 127.2, 126.1, 124.4, 124.2, 124.1, 123.1, 123.0, 122.8, 122.4, 122.3, 122.0, 120.5, 119.4, 112.8, 109.0, 108.8, 95.6, 91.8, 91.4, 89.3, 88.1, 86.6, 44.7, 40.6, 31.8, 29.3, 29.2, 28.1, 27.2, 22.6, 22.3, 14.1, 11.8. MS (FAB; *m*/*z*): 740.9 (M^+). Anal. Calcd for $C_{53}H_{44}N_2O_2$: C, 85.91; H, 5.99; N, 3.78. Found: C, 85.86; N, 6.03; N, 3.60.

2-Octyl-6-{3-[(3-(9-propyl-9*H*-carbazol-3-yl)ethynyl)-phenyl)ethynyl]phenyl)ethynyl}benzo[*de*]isoquinoline-1,3-dione (4). The title compound was obtained in 85% yield from **12** and **8** by following the standard Sonogashira protocol. A yellow solid formed. ^{1}H NMR [δ ($CDCl_3$)]: 0.86 (t, J = 7.3 Hz, 3 H), 0.96 (t, J = 7.3 Hz, 3 H), 1.26−1.42 (m, 10 H), 1.64−1.76 (m, 2 H), 1.84−1.96 (m, 2 H), 4.15 (t, J = 7.3 Hz, 2 H), 4.24 (t, J = 7.3 Hz, 2 H), 7.24 (t, J = 7.7 Hz, 1 H), 7.32−7.41 (m, 4 H), 7.43−7.49 (m, 2 H), 7.53−7.63 (m, 4 H), 7.76−7.84 (m, 3 H), 7.90 (d, J = 7.7 Hz, 1 H), 8.06 (d, J = 7.7 Hz, 1 H), 8.26 (d, J = 1.5 Hz, 1 H), 8.51 (d, J = 7.7 Hz, 1 H), 8.60 (d, J = 6.6 Hz, 1 H), 8.68 (d, J = 6.6 Hz, 1 H). ^{13}C NMR [δ ($CDCl_3$)]: 163.9, 163.6, 140.8, 140.2, 134.8, 134.5, 132.3, 132.2, 131.5, 131.4, 130.8, 130.7, 130.2, 129.2, 128.8, 128.5, 127.9, 127.4, 127.1, 126.1, 124.4, 124.1, 123.8, 123.0, 122.9, 122.8, 122.6, 122.3, 122.2, 120.4, 119.4, 112.7, 108.9, 108.8, 97.9, 91.8, 89.8, 88.6, 44.7, 40.6, 31.8, 29.3, 29.2, 28.1, 27.1, 22.6, 22.3, 14.1, 11.8. MS (EI; *m*/*z*): 740.9 (M^+). Anal. Calcd for $C_{53}H_{44}N_2O_2$: C, 85.91; H, 5.99; N, 3.78. Found: C, 86.12; H, 6.01; N, 3.76.

Measurements. For the spectroscopic measurements, stock solutions of each sample were prepared at the concentration of 3.2×10^{-3} M and further diluted to measure spectra. Samples in solvents such as hexane, toluene, chloroform, tetrahydrofuran (THF), dichloromethane, and *N*,*N*-dimethylformamide (DMF) (Fisher Scientific, spectral grade) were also made to measure absorption and fluorescence spectra and determine the Stokes shifts. Steady-state UV−vis absorption (using a Varian Cary 50 Bio UV−vis spectrophotometer) and fluorescence spectra (using a Jobin Yvon Spex Fluorolog Tau-3 fluorescence spectrophotometer) were measured and quantum yields were determined. Samples were prepared with maximum optical density around 0.1 at the excitation wavelength (357 nm), to minimize self-absorption effects. Cresyl violet perchlorate (Exiton Chemical) solution in methanol (quantum yield 0.54)[32] was used as a standard for the determination of the quantum yields. Fluorescence lifetimes were measured by exciting the same samples with femtosecond pulses centered at 400 nm and collecting the emission at 90°. The fluorescence was focused into a spectrometer (Spectra Pro-150) with a 150 grooves/mm grating to disperse the spectrum before it entered a picosecond time-resolved streak camera (Hamamatsu streak scope C4334). The time resolution of the streak camera is 15 ps, and the spectral resolution is 2 nm. In all cases, the fluorescence spectrum was not observed to undergo any shift or change in shape during its decay, indicating that the emission originated from a single species.

The two-photon absorption fluorescence emission of molecules **1**−**4** in toluene was measured to obtain two-photon absorption cross sections. A tunable Ti:Sapphire femtosecond laser (Spectra Physics Mai Tai, pulse width less than 100 fs and repetition rate 80 MHz) was used to excite the samples over the wavelength range 710−920 nm with an increment of 10 nm. The beam power was attenuated to 90 mW at 800 nm using a neutral density filter. The laser beam was focused into a sample solution in a quartz cell (1 cm path length) using a 35 mm focal length lens, and the resultant two-photon fluorescence emission was collected at right angle with a 50 mm focal length lens. The collected light was detected with a photomultiplier tube (PMT, Hamamatsu R5600U). An optical filter was inserted in front of the PMT to filter out Rayleigh scattering of excitation beam. A chopper (Stanford Research Systems, SR 540) and a lock-in amplifier (SR 830 DSP) were used to remove any stray background signal. The photomultiplier signal was measured over a series of laser powers to confirm its quadratic dependence on laser power, as expected for a two-photon process. Optical filter and PMT responses over the fluorescence wavelengths were measured and used to correct the measured cross sections reported herein.

To calculate the two-photon cross section δ, we used the following equation:[33]

$$\langle F(t)\rangle \approx \frac{1}{2}\phi\eta_2 C\delta\frac{g_p}{f\tau}\frac{8n\langle P(t)\rangle^2}{\pi\lambda} \qquad (1)$$

In this equation, $\langle F(t)\rangle$ is the time-averaged fluorescence photon flux, ϕ is the fluorescence collection efficiency of the measurement system, η_2 is the fluorescence quantum efficiency, δ is the two-photon absorption cross section, and $\langle P(t)\rangle$ is the time-averaged incident laser power. The time-averaged two-photon absorption is proportional to the square of the incident intensity I ($=\langle I_0^2(t)\rangle$), but most detectors detect a signal that is proportional to $\langle I_0(t)\rangle$. Hence g is introduced in eq 1, which is the

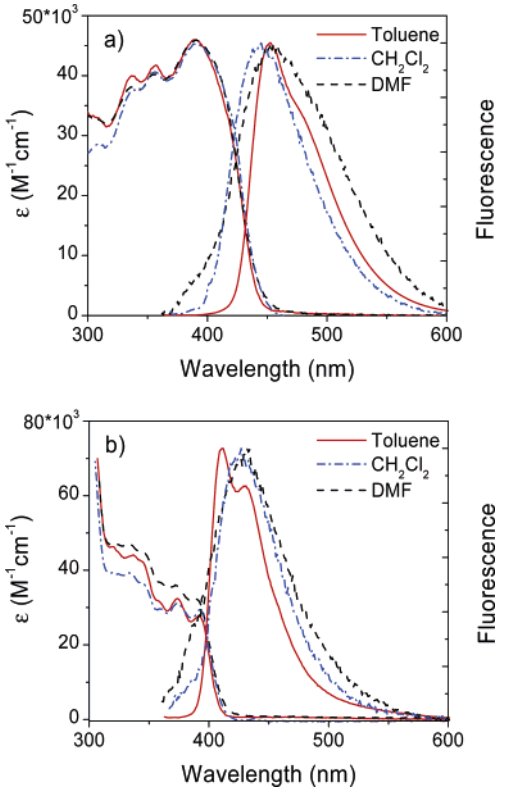

Figure 2. Absorption and fluorescence spectra of molecules (a) **1** and (b) **4** in toluene (solid), dichloromethane (dash−dot), and DMF (dashed). Absorption is in molar extinction coefficient ϵ, and fluorescence is normalized for comparison.

degree of second-order temporal coherence of the excitation source and defined as $\langle I_0^2(t)\rangle/\langle I_0(t)\rangle^2$, where $g = g_p/(f\tau)$, g_p is a dimensionless constant, f is the excitation laser pulse repetition rate, τ is the pulse width (fwhm), and λ is the wavelength of the incident light. C is the concentration of a sample, and n is the refractive index of the solvent, respectively. As we tuned our femtosecond laser source, the wavelength λ, the pulse width τ, and the laser power $\langle P(t)\rangle$ all changed and had to be measured again. We assumed that the pulses were always transform limited, so g_p was constant. The fluorescence collection efficiency of our measurement system was obtained by using Coumarin 307 in methanol as a standard, along with the fluorescence quantum yield of 0.56 in methanol as measured by ourselves and a previous group.[34]

Results and Discussion

The DBA molecules shown in Figure 1 differ only by the number of *meta* versus *para* linkages. For molecules **1**−**4**, the absorption is insensitive to solvent polarity but does depend on the connectivity of the PA linker. The different bridge structures give rise to different absorption spectra, as can be seen in Figure 2 where the most extreme variations, between molecules **1** and **4**, are shown. In the all-*para* bridge, the absorption peaks at 390 nm with a tail extending out to 450 nm, while for the all-*meta* bridge the absorption consists of multiple peaks, the first of which occurs at 391 nm with a steep rise from 420 nm. In all the molecules, the absorption is red-shifted relative to the absorptions of the donor carbazole (365 nm) and the acceptor naphthalimide (345 nm). This red shift and the dependence of the spectral shape on bridge connectivity indicate that the bridge electronic states are involved in the lowest energy electronic transition. The fluorescence spectra are more uniform in appearance and show a slight dependence on solvent polarity.

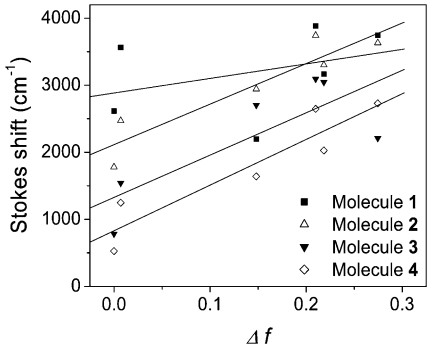

Figure 3. Lippert−Mataga plot for molecules **1**−**4**. Δf, the orientation polarizability, is defined by $\Delta f = (\epsilon - 1)/(2\epsilon + 1) - (n^2 - 1)/(2n^2 + 1)$ in eq 2. The data points represent hexane, toluene, chloroform, THF, dichloromethane, and DMF in the order of increasing Δf. Solvent properties used to calculate Δf were obtained from the *CRC Handbook of Chemistry and Physics*, 76th ed.

Figure 2 shows the fluorescence spectra for **1** and **4** in toluene, CH_2Cl_2, and DMF. In toluene, for all molecules, the fluorescence has a small Stokes shift and exhibits vibronic features, as expected for a neutral excited state. As the solvent becomes more polar, the emission shifts and broadens. The most dramatic effect is a precipitous drop in quantum yield in more polar solvents, suggesting that the fluorescence is being quenched by an intramolecular electron transfer which becomes more favorable in polar solvents. To avoid this complication, we performed all our two-photon measurements in toluene, the least polar solvent. The other information we can obtain from the steady-state spectroscopy is the amount of charge-transfer character of the excited state. By plotting the fluorescence Stokes shift versus the solvent dielectric field, as shown in Figure 3, we can extract the change in dipole moment $\Delta\mu_{01}(=\mu_E - \mu_G)$ upon going from the ground to the excited state using the Lippert−Mataga formula:

$$\bar{\nu}_A - \bar{\nu}_F = \frac{2}{hc}\left(\frac{\epsilon - 1}{2\epsilon + 1} - \frac{n^2 - 1}{2n^2 + 1}\right)\frac{(\mu_E - \mu_G)^2}{a^3} + \text{constant} \quad (2)$$

Here $\bar{\nu}_A$ and $\bar{\nu}_F$ are the peaks (cm^{-1}) of the absorption and emission, respectively, n and ϵ are the refractive index and the dielectric constant of the solvent, respectively, h is Planck's constant, c is the speed of light, and a is the radius of the cavity in which the fluorophore resides. In eq 2, the molecular radius a is an undetermined parameter. One way to calculate it is to add up the volumes of the chemical groups in the molecule and then assume the total volume is contained in a sphere whose radius can then be calculated.[35,36] However, since molecules **1**−**4** possess the same chemical groups, they all have the same volume and thus would have the same radius a as well. To more closely approximate the actual molecular radius, we use PM3 molecular mechanics simulations to obtain molecular conformations and then calculate the end-to-end distances. The choice of the end point is somewhat arbitrary, and in this work we take it to be the distance between the carbazole nitrogen and the middle of the naphthalimide ring. Using other metrics, for example the distance between the terminal bridge carbons, did not significantly change our results. These distances, along with the $\Delta\mu$ values obtained from the Lippert−Mataga plots, are given in Table 1. Also shown in Table 1 are the fluorescence quantum yields and decay characteristics for molecules **1**−**4**, along with the molecules' steady-state characteristics in toluene. These values will be used in subsequent calculations of the relative two-photon cross sections.

TABLE 1: Spectral Properties of Molecules 1−4 in Toluene

property	1	2	3	4
abs peaks, λ_{abs} (nm)	390	374	405	391
lifetimes[a]	1.3 ns	47 ps, 5.6 ns	1.4 ns	0.46 ns
quantum yields[b]	1.00	0.49	1.03	0.14
$M_{01}^2 \propto \epsilon$ (M^{-1} cm^{-1})	45 984	63 690	35 898	27 724
a (Å)	24.365	21.194	21.484	19.106
$\Delta\mu_{01}$ (D)	55.8	45.3	46.2	38.8
δ (GM; measured at λ (nm))	120 (790)	98 (750)	44 (820)	15 (790)

[a] Lifetime of molecule **2** was fitted as biexponential with prefactors of 0.67 and 0.33 for the time coefficients of 47 ps and 5.6 ns, respectively. [b] Quantum yields are within ±10% error.

In Figure 4 we show the measured two-photon absorption line shapes, shifted to twice the photon energy so that they overlap the one-photon spectra. The two-photon absorption measurements are consistent with the one-photon allowed state being the dominant contributor to the two-photon absorption. In all four cases, the two spectra are very similar, even down to the small vibronic peaks observed for molecule **4** in Figure 4d. But while the peak ϵ's for molecules **1**−**4** are within a factor of 2 of each other, the two-photon cross sections δ differ by a factor of 10. The all-*para* molecule **1** has the largest $\delta = 120$ GM (1 GM = $(1 \times 10^{-50}$ cm^4 s/photon)/molecule). This high δ, along with its fluorescence quantum yield of unity, would make the molecule a reasonable candidate for fluorescence labeling applications. As the number of *meta* linkages increases, however, δ decreases, until we have molecule **4**, whose $\delta =$ 15 GM is almost a factor of 10 lower than **1**'s.

The similarity of the one- and two-photon spectra indicates that our molecules can be understood within the framework of the two-state model[25,37] which has successfully been used to predict trends in other classes of dipolar two-photon absorbers.[38] Previous workers have shown that this model does a good job of predicting how δ varies with changes in chemical structure. In almost all cases, such changes have consisted in varying the donor/acceptor moieties rather than the bridge. The equation that describes the imaginary part of the second-order hyperpolarizability γ in terms of the ground and first excited states is given by[25,38]

$$\mathrm{Im}\,\gamma = \frac{4}{5}\,\mathrm{Im}\left[\frac{M_{01}{}^2(\Delta\mu_{01}{}^2)}{(E_{01} - \hbar\omega - \mathrm{i}\Gamma_{01})^2(E_{01} - 2\hbar\omega - \mathrm{i}\Gamma_{01})}\right] \quad (3)$$

This γ then determines the two-photon absorption cross section δ through the relation

$$\delta(\omega) = \frac{4\pi^2\hbar\omega^2}{n^2c^2} L^4\,\mathrm{Im}\,\gamma(-\omega;\omega;-\omega,\omega) \quad (4)$$

In these equations, M_{01} is the transition dipole moment for the $S_0 \rightarrow S_1$ excitation, $\Delta\mu_{01}$ is the difference in dipole moment between S_1 and S_0, E_{01} is the excitation energy for the $S_0 \rightarrow S_1$ transition, $\hbar\omega$ is excitation energy, Γ is a damping factor (set to 0.1 eV), L is Lorentz field correction, $L = (n^2 + 2)/3$, n is the refractive index of solvent, and c is the velocity of light. The values used to calculate the two-photon absorption spectra for molecules **1**−**4** are given in Table 1. We have assumed that M_{01}^2 is directly proportional to the peak value of the linear absorption coefficient ϵ in Table 1. This is an approximation, since in general the peak ϵ depends both on M_{01}^2 and on the absorption line width,[39] and there is no guarantee that the line width is the same for molecules **1**−**4**. For example, the lower ϵ for the fully conjugated molecule **1** relative to **2** is unexpected, since extended conjugation is usually thought to give rise to a larger transition dipole. This discrepancy may be due to different amounts of line broadening in the molecules. Deriving an unequivocal line width is a difficult task, however, given the overlapping absorptions shown in Figure 2. As shown below, our approach to estimating M_{01}^2 leads to satisfactory results, despite its simplicity. We plot the measured values of δ for compounds **1**−**4** in Figure 5, along with the calculated δ's obtained from using the values in Table 1 and eqs 3 and 4. Note that we use the δ values for the lowest energy peaks in the two-photon absorption spectra to avoid the possibility of contributions from higher lying excited states. The calculated δ's have all been scaled by an arbitrary constant so that the trends in relative values may be compared. The simple two-level theory appears to capture the general trend of the decreasing δ with increasing numbers of *meta* links. From Table 1, we see that the main term that drives this decrease in δ is the decreasing $\Delta\mu^2$ term. This is at first surprising, since **4** actually shows a more dramatic solvatochromic shift than **1**, which at first glance would seem to imply a larger $\Delta\mu$. But this large shift is due to a smaller molecular radius a which enhances the solvent field rather than a larger amount of charge-transfer character. This fact shows the importance of taking the molecular conformation into account in our data analysis.

The ability of *meta* linkages to inhibit charge transfer and thus decrease δ is not unexpected.[24] The effects of ground-state conjugation on molecular nonlinear optical properties is well-established, both experimentally and theoretically. Experimentally, Prasad and co-workers observed that fixing conjugated rings within a plane increased γ by a factor of 3 in fluorene-bridged compounds.[22] They interpreted their results qualitatively in terms of planarizing the bridge and improving the conjugation across it. There is also direct theoretical evidence for the effect of conformation on δ.[40] Different bonding arrangements or the substitution of heteroatoms can also affect conjugation through a bridge. Evidence for the influence of π-electron bond conjugation on the nonlinear susceptibility can be found in numerous theoretical studies.[41−43] In these cases, the influence of conjugation on the polarizability was found by calculating the effect for specific examples, and to our knowledge there does not exist a general formula which relates conjugation to nonresonant nonlinear optical properties. Also, in many of these studies the effects are relatively small, as opposed to the order of magnitude change observed here. One experimental study looked at the effect of substituting nitrogen atoms into a fixed bridge structure and concluded that the bridge had little effect on the measured two-photon intensities.[44]

To interpret the results for molecules **1**−**4**, we first consider previous work on PA dendrimers which assumed that *meta* substitution completely prevents electronic delocalization in the ground-state configuration.[45] Even if a single *meta* linkage completely prevented electronic communication, we would still expect each molecule to exhibit a different δ. This is because each *meta* link would effectively divide the molecule into two parts, each of which has its own contribution to δ due to the donor (acceptor) electronic states extending a variable distance into the bridge. For example, molecules **2** and **3** have different δ values, despite their identical bridge structures. From the data in Table 1, the enhanced δ for **2** relative to **3** is a direct result of its large absorption coefficient, which itself is likely due to better conjugation of the naphthalimide ring to the PA bridge. However, if the *meta* linkage really cut off the donor entirely from the acceptor, then we would expect to see a precipitous drop in δ as we go from zero to one *meta* linkage rather than

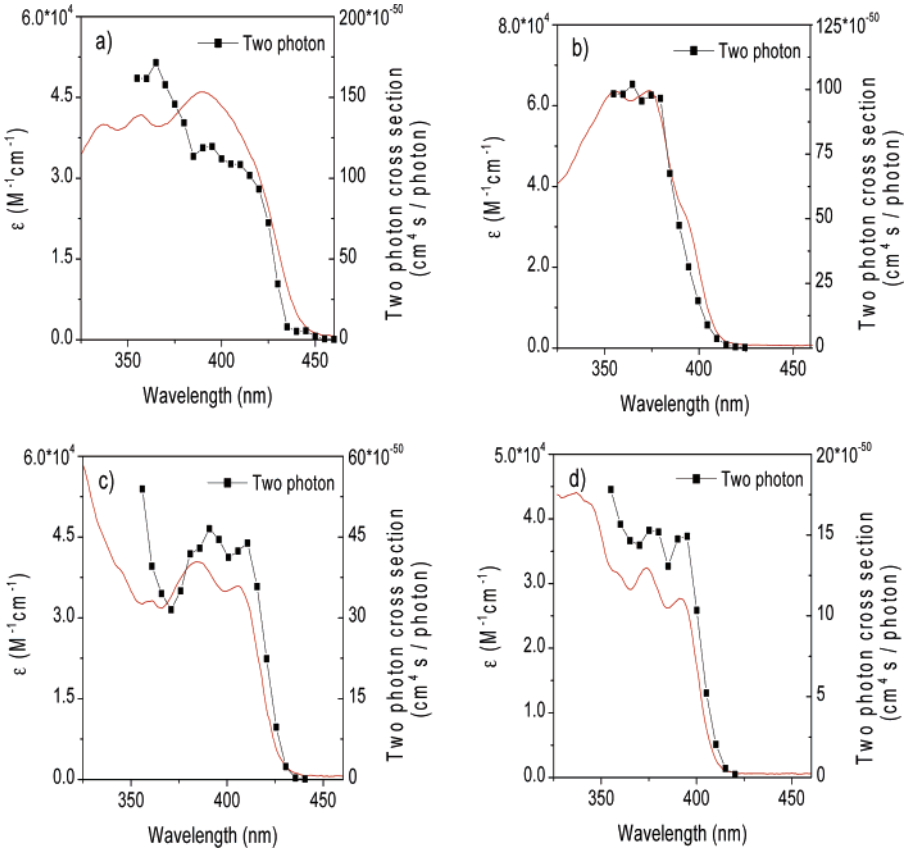

Figure 4. (a−d) Comparison of one-photon (solid line) and two-photon (squares) absorption spectra of molecules **1**−**4** in toluene. The measured two-photon absorption line shapes are shifted to twice the photon energy so that they overlap the one-photon spectra.

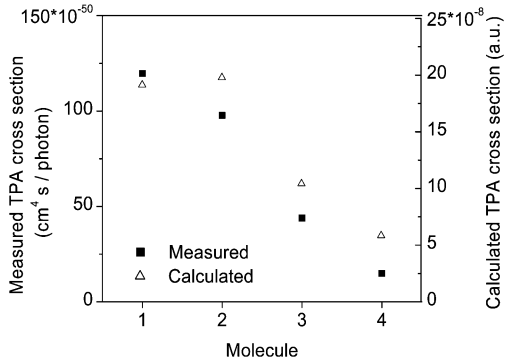

Figure 5. Plot of measured (solid squares) and calculated (triangles) two-photon absorption cross sections δ versus the number of *meta* links in molecules **1**−**4** in toluene. The calculated δ's have been scaled by an arbitrary factor for comparison with the experimental δ's.

the quasi-linear decrease in δ with additional *meta* links. From Table 1, this steady decrease in δ reflects a more gradual decrease in $\Delta\mu$ with increasing *meta* conjugation. The electron-transfer ability of *para*- versus *meta*-linked phenylene,[46−48] phenylenevinylene,[49] and PA[50,51] linkers has been investigated. In the excited state, there is evidence that the charge-transfer interactions can be enhanced, although such enhancement only occurs after vibrational relaxation on the excited-state potential energy surface and thus would not be expected to play a role in the instantaneous nonresonant two-photon absorption event. The largest error in our use of eqs 3 and 4 to predict δ lies in our estimate of $\Delta\mu$ from the Lippert−Mataga plots. We interpreted our results in terms of a charge separation across the entire bridge but whose magnitude decreases with increasing *meta* conjugation. In other words, *meta* conjugation leads to less charge being transferred over the same number of bonds. An alternate explanation might be that the amount of charge which separates is always the same but that the distance over which it occurs is limited by the first *meta* linkage which is encountered, i.e., that the *meta* linkages completely prevent electronic communication across the bridge. In this case, however, the scaling of a with molecule becomes much more dramatic, and the $\Delta\mu$'s would show even more variation. Rather than slightly underestimating the observed decrease of δ with the number of *meta* links, the theory would now overestimate it by at least a factor of 2. In the present case, our data analysis indicates that the two-photon cross section δ is a sensitive measure of how *meta* conjugation prevents electronic communication across the entire bridge, providing a way to quantify this effect as a function of the number of "kinks" in the PA wire.

Two additional comments are in order. First, our analysis assumes that static structural factors determine the relative δ's in this series of molecules. Of course, dynamic factors may affect the absolute δ values in **1**−**4**. The barrier to rotation around the triple bond is on the order of 1 kcal/mol in phenylacetylene chains,[52−55] so it is likely that these bridge structures are undergoing significant torsional motion at room temperature. Since all four molecules will experience a similar level of rotational fluctuations, this dynamic effect is expected to affect them more or less equally, lowering all the δ's by a similar factor. The effect of rotational motion on δ could be tested by designing bridge structures that lock in a planar bridge conformation or by measuring δ in a low-temperature rigid matrix. The second point is that although the simple theory does a good job of predicting the qualitative dependence of δ on the number of meta links, it appears to underestimate this effect. This can be seen from Figure 5, where the calculated δ for **4** is two times larger than the measured δ. It may be that our simple spherical cavity model is insufficient to describe the complicated

geometry of these compounds. Improved cavity models, which take the nonspherical aspects of the molecular geometry into account,[56] might remove some of the remaining discrepancy between theory and experiment. But considering the simplicity of the model, the overall agreement between experiment and theory is surprisingly good.

Conclusion

In this work, we have studied the linear and nonlinear optical properties of a class of four isoelectronic donor−bridge−acceptor compounds with different bridge connectivities. As the number of *meta* links in the PA bridge increases from 0 to 2, the two-photon absorption cross section decreases by almost 1 order of magnitude. This dependence of δ on the bridge conjugation is described semiquantitatively by a simple two-state theory of two-photon absorption for dipolar compounds, which predicts the two-photon behavior on the basis of the resonant one-photon spectroscopic properties. The key part in the application of this theory is the use of realistic molecular conformations to obtain accurate $\Delta\mu$ values. From our results, one can estimate that each additional *meta* linkage reduces the two-photon absorption cross section by about a factor of 3, mainly due to the decreased ability of the ground-state bridge to support charge transfer between the donor and acceptor moieties.

Acknowledgment. This work was supported by the Department of Energy, Office of Basic Energy Sciences, Grants DEFG02-1ER15720 and DEFG-02ER15503.

Note Added after ASAP Publication. The zipcode was added to the author address and acronym (DBA) was added to define donor−bridge−acceptor. This paper was published ASAP on 10/8/05. The corrected version was posted on 10/10/05.

References and Notes

(1) Kanis, D. R.; Ratner, M. A.; Marks, T. J. *Chem. Rev.* **1994**, *94*, 195−242.
(2) Brédas, J.-L.; Adant, C.; Tackx, P.; Persoons, A. *Chem. Rev.* **1994**, *94*, 243−278.
(3) Mukamel, S.; Takahashi, A.; Wang, H. X.; Chen, G. *Science* **1994**, *266*, 250−254.
(4) Dalton, L. R. *J. Phys. Cond. Mater.* **2003**, *15*, R897−R934.
(5) Strickler, J. H.; Webb, W. W. *Opt. Lett.* **1991**, *16*, 1780−1782.
(6) Olson, C. E.; Previte, M. J. R.; Fourkas, J. T. *Nat. Mater.* **2002**, *1*, 225−228.
(7) Blefield, K. D.; Schafer, K. J. *Chem. Mater.* **2002**, *14*, 3656−3662.
(8) Cumpston, B. H.; Ananthavel, S. P.; Barlow, S.; Dyer, D. L.; Ehrlich, J. E.; Erskine, L. L.; Heikal, A. A.; Kuebler, S. M.; Lee, I. Y. S.; McCord-Maughon, D.; Qin, J.; Rockel, H.; Rumi, M.; Wu, X.-L.; Marder, S. R.; Perry, J. W. *Nature* **1999**, *398*, 51−54.
(9) Blefield, K. D.; Ren, X.; Stryland, E. W. V.; Hagan, D. J.; Dubikovsky, V.; Miesak, E. J. *J. Am. Chem. Soc.* **2000**, *122*, 1217−1218.
(10) Zhou, W.; Kuebler, S. M.; Braun, K. L.; Yu, T.; Cammack, J. K.; Ober, C. K.; Perry, J. W.; Marder, S. R. *Science* **2002**, *296*, 1106−1109.
(11) Coenjarts, C. A.; Ober, C. K. *Chem. Mater.* **2004**, *16*, 5556−5558.
(12) LaFratta, C. N.; Baldacchini, T.; Farrer, R. A.; Fourkas, J. T.; Teich, M. C.; Saleh, B. E. A.; Naughton, M. J. *J. Phys. Chem. B* **2004**, *108*, 11256−11258.
(13) Teh, W. H.; Durig, U.; Salis, G.; Harbers, R.; Drechsler, U.; Mahrt, R. F.; Smith, C. G.; Guntherodt, H.-J. *Appl. Phys. Lett.* **2004**, *84*, 4095−4097.
(14) Karotki, A.; Dobrizhev, M. A.; Kruk, M.; Rebane, A.; Nickel, E.; Spangler, C. W. *IEEE J. Sel. Top. Quantum Electron.* **2001**, *7*, 971−975.
(15) Dichtel, W. R.; Serin, J. M.; Edder, C.; Frechet, J. M. J.; Matuszewski, M.; Tan, L.-S.; Ohulchanskyy, T. Y.; Prasad, P. N. *J. Am. Chem. Soc.* **2004**, *126*, 5380−5381.
(16) Denk, W.; Strickler, J. H.; Webb, W. W. *Science* **1990**, *248*, 73−76.
(17) Piston, D. W.; Bennett, B. D.; Ying, G. *J. Microsc. Soc. Am.* **1995**, *1*, 25−34.
(18) Xu, C.; Zipfel, W.; Shear, J. B.; Williams, R. B.; Webb, W. W. *Proc. Nat. Acad. Sci. U.S.A.* **1996**, *93*, 10763−10768.
(19) Rumi, M.; Ehrlich, J. E.; Heikal, A. A.; Perry, J. W.; Barlow, S.; Hu, Z.; McCord-Maughon, D.; Parker, T. C.; Rockel, H.; Thayumanavan, S.; Marder, S. R.; Beljonne, D.; Brédas, J.-L. *J. Am. Chem. Soc.* **2000**, *122*, 9500−9510.
(20) Albota, M.; Beljonne, D.; Brédas, J.-L.; Ehrlich, J. E.; Fu, J.-Y.; Heikal, A. A.; Hess, S. E.; Kogej, T.; Levin, M. D.; Marder, S. R.; McCord-Maughon, D.; Perry, J. W.; Rockel, H.; Rumi, M.; Subramaniam, G.; Webb, W. W.; Wu, X.-L.; Xu, C. *Science* **1998**, *281*, 1653−1656.
(21) Kannan, R.; He, G. S.; Yuan, L.; Xu, F.; Prasad, P. N.; Dombroskie, A. G.; Reinhardt, B. A.; Baur, J. W.; Vaia, R. A.; Tan, L.-S. *Chem. Mater.* **2001**, *13*, 1896−1904.
(22) Reinhardt, B. A.; Brott, L. L.; Clarson, S. J.; Dillard, A. G.; Bhatt, J. C.; Kannan, R.; Yuan, L.; He, G. S.; Prasad, P. N. *Chem. Mater.* **1998**, *10*, 1863−1874.
(23) Ventelon, L.; Charier, S.; Moreaux, L.; Mertz, J.; Blanchard-Desce, M. *Angew. Chem., Int. Ed.* **2001**, *40*, 2098−2101.
(24) Meyers, F.; Marder, S. R.; Pierce, B. M.; Brédas, J.-L. *J. Am. Chem. Soc.* **1994**, *116*, 10703−10714.
(25) Kogej, T.; Beljonne, D.; Meyers, F.; Perry, J. W.; Marder, S. R.; Brédas, J.-L. *Chem. Phys. Lett.* **1998**, *298*, 1−6.
(26) Zojer, E.; Beljonne, D.; Pacher, P.; Brédas, J.-L. *Chem.*—Eur. J. **2004**, *10*, 2668−2680.
(27) Katan, C.; Terenziani, F.; Mongin, O.; Werts, M. H. V.; Porres, L.; Pons, T.; Mertz, J.; Tretiak, S.; Blanchard-Desce, M. *J. Phys. Chem. A* **2005**, *106*, 3024−3037.
(28) Barzoukas, M.; Blanchard-Desce, M. *J. Chem. Phys.* **2000**, *113*, 3951−3959.
(29) Baev, A.; Prasad, P. N.; Samoc, M. *J. Chem. Phys.* **2005**, *122*, 224309/ 1−224309/6.
(30) Spanggaard, H.; Jorgensen, M.; Almdal, K. *Macromolecules* **2003**, *36*, 1701−1705.
(31) Holtrup, F. O.; Muller, G. R. J.; Quante, H.; Defeyter, S.; DeSchryver, F. C.; Mullen, K. *Chem.*—Eur. J. **1997**, *3*, 219−225.
(32) Magde, D.; Brannon, J. H.; Cremers, T. L.; Olmstead, J. *J. Phys. Chem.* **1979**, *83*, 696−699.
(33) Xu, C.; Webb, W. W. *J. Opt. Soc. Am. B* **1996**, *13*, 481−491.
(34) Reynolds, G. A.; Drexhage, K. H. *Opt. Commun.* **1975**, *13*, 222−225.
(35) Maroncelli, M.; Fleming, G. R. *J. Chem. Phys.* **1987**, *86*, 6221−6239.
(36) Edward, J. T. *J. Chem. Educ.* **1970**, *47*, 261−270.
(37) Dick, B.; Hohlneicher, G. *J. Chem. Phys.* **1982**, *76*, 5755−5760.
(38) Strehmel, B.; Sarker, A. M.; Detert, H. *Chem. Phys. Chem.* **2003**, *4*, 249−259.
(39) Allen, L.; Eberly, J. H. *Optical Resonance and Two-Level Atoms*; Dover: New York, 1987.
(40) Pati, S. K.; Marks, T. J.; Ratner, M. A. *J. Am. Chem. Soc.* **2001**, *123*, 7287−7291.
(41) Andre, J.-M.; Dehalle, J. *Chem. Rev.* **1991**, *91*, 843−865.
(42) Nalwa, H. S.; Mukai, J.; Kakuta, A. *J. Phys. Chem.* **1995**, *99*, 10766−10774.
(43) Shuai, A.; Ramasesha, S.; Brédas, J.-L. *Chem. Phys. Lett.* **1996**, *250*, 14−18.
(44) Antonov, L.; Kamada, K.; Ohta, K.; Kamounah, F. S. *Phys. Chem. Chem. Phys.* **2003**, *5*, 1193−1197.
(45) Kopelmann, R.; Shortreed, M.; Shi, Z.; Tan, W.; Xu, Z.; Moore, J. S.; Bar-Haim, A.; Klafter, J. *Phys. Rev. Lett.* **1997**, *78*, 1239−1242.
(46) Stockmann, A.; Kurzawa, J.; Fritz, N.; Acar, N.; Schneider, S.; Daub, J.; Engl, R.; Clark, T. *J. Phys. Chem. A* **2002**, *106*, 7958−7970.
(47) Tkachenko, N. V.; Lemmetyinen, H.; Sonoda, J.; Ohkubo, K.; Sato, T.; Imahori, H.; Fukuzumi, S. *J. Phys. Chem. A* **2003**, *107*, 8834−8844.
(48) Shaakov, S.; Galili, T.; Stavitski, E.; Levanon, H.; Lukas, A.; Wasielewski, M. R. *J. Am. Chem. Soc.* **2003**, *125*, 6563−6572.
(49) Rovira, C.; Ruiz-Molina, D.; Elsner, O.; Vidal-Gancedo, J.; Bonvoisin, J.; Launay, J.-P.; Veciana, J. *Chem.*—Eur. J. **2001**, *7*, 240−250.
(50) Gaab, K. M.; Thompson, A. L.; Xu, J.; Martinez, T. J.; Bardeen, C. J. *J. Am. Chem. Soc.* **2003**, *125*, 9288−9289.
(51) Thompson, A. L.; Gaab, K. M.; Xu, J.; Bardeen, C. J.; Martinez, T. J. *J. Phys. Chem. A* **2004**, *108*, 671−682.
(52) Sluch, M. I.; Godt, A.; Bunz, U. H. F.; Berg, M. A. *J. Am. Chem. Soc.* **2001**, *123*, 6447−6448.
(53) Beeby, A.; Findlay, K.; Low, P. J.; Marder, T. B. *J. Am. Chem. Soc.* **2002**, *124*, 8280−8284.
(54) Levitus, M.; Schmieder, K.; Ricks, H.; Shimizu, K. D.; bunz, U. H. F.; Garcia-Garibay, M. A. *J. Am. Chem. Soc.* **2001**, *123*, 4259−4265.
(55) Levitus, M.; Schmieder, K.; Ricks, H.; Shimizu, K. D.; Bunz, U. H. F.; Garcia-Garibay, M. A. *J. Am. Chem. Soc.* **2002**, *124*, 8181−8181.
(56) Morales-Lagos, D.; Gomez-Jeria, J. S. *J. Phys. Chem.* **1991**, *95*, 5308−5314.